

Effect of Chitosan Loading on Mechanical Properties, Water Uptake and Toluene Absorbency of High and Low Molecular Weight ENR50

GUNA SUNDERI RAJU^{*,**}, MAS ROSEMAL HAKIM MAS HARIS^{*#}, A.R. AZURA^{***},
A. BAHARIN^{****} AND N. KARTINI^{*****}

This paper reports preparation, mechanical properties, water uptake and toluene absorbency of biocomposites comprising different loadings of chitosan (CTS) (5, 10, 15, 20 and 30 p.h.r.) into matrixes of ENR50 and LENR50 (high and low molecular weight epoxidised natural rubbers with epoxy content of about 50%, respectively). It is found that the increase in CTS loading increased cure torque, tensile strength and modulus at 100% but there was a decline in cure time and elongation at break for CTS-ENR50 biocomposites. Similar trends were observed for CTS-LENR50 biocomposites except for cure torque and tensile strength, with no significant changes upon increase in CTS loading. SEM micrographs of the tensile-fractured materials showed that at 15 p.h.r. loading, for example, CTS underwent a breakout, indicating good interactions in the CTS-ENR50 biocomposites. TGA data revealed that thermal stability of both CTS-ENR50 and CTS-LENR50 biocomposites remained fairly close to that of their respective unloaded rubber matrix. Results of the water uptake study revealed that increase in CTS loading led to an increase in water uptake of CTS-LENR50 biocomposites, found to be considerably higher at every loading compared with that of CTS-ENR50 biocomposites. Results of the toluene absorbency study revealed that LENR50 is a superior sorbent for toluene compared to ENR50. However, increase in CTS loading led to a decrease in toluene absorbency of both CTS-LENR50 and CTS-ENR50 biocomposites.

Keywords: epoxidised natural rubber; chitosan; biocomposites; mechanical properties; water uptake; toluene absorbency

Epoxidised natural rubber (ENR) is a derivative of natural rubber (NR) with epoxide moiety distributed randomly on the backbone of the polymer as well as specific properties

compared to that of NR such as better oil resistance and air permeability¹⁻³. Currently, ENR with the epoxy contents of about 25% and 50% (designated as ENR25 and ENR50,

* School of Chemical Sciences, Universiti Sains Malaysia, 11800 Minden, Pulau Pinang

** Rubber Research Institute of Malaysia, Malaysian Rubber Board, P.O. Box 10150, K. Lumpur, Malaysia.

*** School of Materials and Mineral Resources Engineering, Universiti Sains Malaysia, 14300 Nibong Tebal, Pulau Pinang

**** School of Industrial Technology, Universiti Sains Malaysia, 11800 Minden, Penang, Malaysia

***** Advanced Materials Research Centre (AMREC) SIRIM Berhad, 09000 Kulim Kedah

Corresponding author (e-mail: mas1@usm.my)

respectively) are available commercially⁴. Low molecular weight ENR, commonly referred to as low molecular weight epoxidised natural rubber (LENR), can be obtained *via* depolymerisation of ENR latex⁵. *Figure 1* depicts the general structures and an outline of the preparation of ENR and LENR from NR.

In order to increase the marketability of ENR and its derivatives, numerous efforts are being made to diversify their applications. Blending of ENR with other polymeric materials, such as palm oil wood flour⁶, rice husk ash⁷ and organoclay⁸ is one of the easiest and low cost means for obtaining polymeric materials with better and wider applications. There are also several reports on the preparation of new and useful polymers *via* ring-opening reaction of the epoxy group of ENR⁹⁻¹¹.

Chitosan is a biopolymer consisting of a (1→4)-linked 2-amino-2-deoxy-p-D-glucopyranose obtained from N-deacetylation of chitin that is commonly found in crustacean¹²⁻¹³. The use of natural fillers, such as chitosan, offers several advantages over inorganic fillers with regards to their lower density, reduced abrasiveness to processing equipment, lower cost, inherent biodegradability and environmental friendliness. However, a literature survey reveals that there are a limited number of reports pertaining to the incorporation of chitosan in ENR⁵⁰¹⁴ and ENR25¹⁵⁻¹⁶ to form CTS-ENR biocomposites.

To date, there is no report on the preparation and properties of CTS-LENR50 biocomposites. As such, the preparation and

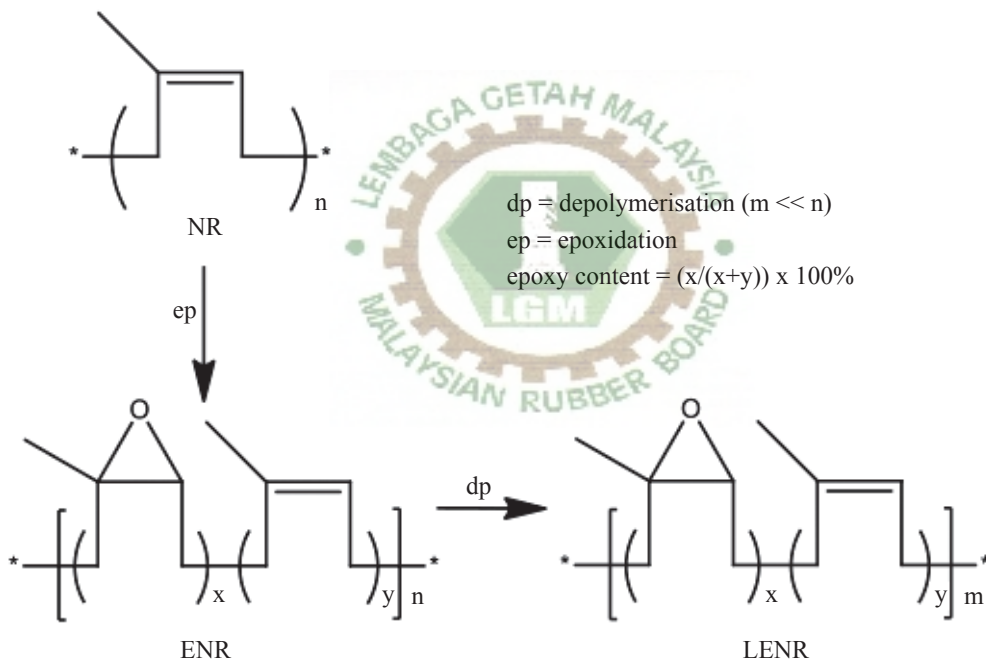


Figure 1. Outline of the preparation of ENR and LENR from natural rubber.

comparison of not only mechanical properties, but also water uptake and toluene absorbency of CTS-ENR50 and CTS-LENR50 biocomposites are reported in this paper.

EXPERIMENTAL

Materials

Epoxidised natural rubber latex with an epoxy content of about 50% (ENR50) and weight average molecular weight of 3.8×10^5 Da was supplied by the Malaysian Rubber Board. The actual epoxy content determined by NMR spectroscopy¹⁷ using a Bruker Avance-400 NMR spectrometer was found to be 51%. Chitosan (% degree of deacetylation; DD \approx 90) was provided by Advanced Materials Research Centre, Kulim Kedah. The weight average molecular weight of the CTS was determined by Size Exclusion Chromatography (SEC) as 1.0×10^5 Da. The SEC analysis for ENR50, CTS and LENR50 was made by a TOSOH SEC, consisting of a TOSOH CCPD pump, RI-8012 Differential Refractometer and UV-8011 UV detector. The other compounding ingredients used were zinc oxide, stearic acid, N-cyclohexyl-2-benzothiazole sulphenamide (CBS) and sulphur, which were all purchased from Bayer Ltd and used as received. Toluene was purchased from Baker Aldrich (M) Ltd. Sodium hydroxide, sodium nitrite, hydrogen peroxide and methanol were purchased from System Chemar, while teric acid (Huntsman Corporation Australia Pty Limited) was supplied by the Malaysian Rubber Board.

Preparation of LENR50

The method described by Gazeley⁵ was adopted with some modifications. A typical procedure is as follows: Teric acid (9 g) was dissolved in water (85.0 mL) and the solution

was added into a conical flask containing ENR50 latex (500 mL) and stirred for 24 hours. Then, the pH of the latex was determined and adjusted with 20% v/v formic acid until a pH of 5 to 5.6 was attained. Subsequently, a sodium nitrite solution (10 g in 35.5 mL water) was added dropwise. Once the addition was completed, the temperature of the latex sample was increased to 50°C and stirred for 15 minutes. Then hydrogen peroxide (83.5 mL of 30%) was added dropwise. After addition of hydrogen peroxide, the latex sample was stirred for a further 15 min before its pH was adjusted if necessary, with 20% v/v formic acid to a pH of 5 to 5.6. After stirring for another 24 h, 10% w/v of sodium hydroxide solution was then added to increase the pH to about 8 to 9. The resulting latex sample was poured into a suitable sized beaker containing methanol and the coagulated material (LENR50) was washed with an ample amount of distilled water. The LENR50 obtained was then freeze-dried. The average molecular weight and epoxy content of the LENR50 were determined to be 1.5×10^5 Da and 51%, respectively.

Preparation of CTS-ENR50 and CTS-LENR50 Biocomposites

Melt blending was carried out at 80°C and 50 r.p.m. rotor speed in a HAAKE Rheomixer mixing chamber. The blending was carried out as follows: When the desired temperature was reached, ENR50 or LENR50 was charged into the mixing chamber and mixed for 1 min before the CTS was added. All ingredients, as shown in *Table 1* except sulphur, were added after 3 min and the blending process was continued for a further 2 minutes. Finally, sulphur was added and the blending process was continued for 1 min before the mixture was dumped and cooled to room temperature to obtain the product (CTS-ENR50 or CTS-LENR50 biocomposite). The cure characteristics of CTS-ENR50 or CTS-LENR50 biocomposite

TABLE 1. FORMULATION OF CTS-ENR50 AND CTS-LENR50 BIOCOMPOSITES

Compounding Ingredients	Content (p.h.r.) ^b
Rubber ^a	100
Chitosan	0, 5, 10, 15, 20, 30
Zinc oxide	3
Sulphur	1.5
N-Cyclohexyl-2-benzothiazole sulphenamide	1
Stearic acid	2

^a ENR50 or LENR50

^b parts per hundred rubber

were determined using a model MDR 2000 Moving Die Rheometer (Alpha Technologies, Swindon, UK) at 150°C in accordance with the Test Method *ASTM D-2084*. Compression moulded sheets (2 mm thick) were prepared and cured at their respective cure times t_{90} .

Mechanical, Morphological and Thermal Properties

Tensile test was done in accordance with *ASTM D638* at room temperature using a computerised tensile tester (Instron IX3366) with a load cell of 10 kN. The crosshead speed of the Instron machine was set at 500 mm/min. The tensile fractured surfaces of samples (CTS-ENR50 and CTS-LENR50 biocomposites) were examined using a Variable Pressure Scanning Electron Microscopy (VPSEM). For the thermogravimetric analysis of the samples, a Perkin Elmer Diamond TG/DTG was used. The heating rate was 10°C min⁻¹ and the sample was heated from 40°C to 600°C in a nitrogen atmosphere. The typical weight of samples used was about 10 mg.

Water Uptake Study

The water absorption test was performed according to the *ASTM D570-95* standard.

The test specimens in rectangular bars were 30 mm long, 5 mm wide and 2 mm thick. The samples (CTS-ENR50 and CTS-LENR50 biocomposites) were immersed in water at room temperature inside a closed bottle. The samples were removed from the water after a 48 h interval, wiped with a dry cloth and weighed to the nearest 0.001 g immediately. The weight was measured until it became nearly constant. For comparison, this experiment was also carried out with ENR50, LENR50 and CTS. Experiments were also carried out for 72 h and it was found that there is no marked variation in the results compared to that of 48 hours. Therefore, this data is accepted as thermodynamic data. The formula used to calculate the percentage of water uptake is shown in *Equation 1*.

$$\text{Percentage of water uptake} = \frac{W_i - W_o}{W_o} \times 100\% \quad \dots 1$$

Where w_o = Initial weight of the sample before immersion in water
 w_i = Weight of wet sample

Toluene Absorbency

Determination of toluene absorbency (swelling index in toluene) of CTS-ENR50 and CTS-LENR50 biocomposites was done

at room temperature. The test specimens in rectangular bars were 30 mm long, 5 mm wide and 2 mm thick. Weight of the samples was measured before immersing into toluene for 72 h and that value taken as the original weight. Samples were then removed from the solvent, wiped to remove excessive solvent on the surface and reweighed. This value was taken as the swollen weight. For comparison, this experiment was also carried out with ENR50, LENR50 and CTS. Toluene absorbency was calculated using *Equation 2*.

$$\text{Percentage of toluene absorbency} = \frac{s_1 - s_o}{s_o} \times 100\% \quad \dots 2$$

Where s_o = Initial weight of the sample before immersion in toluene

s_1 = Weight of swollen sample

RESULTS AND DISCUSSION

Cure Characteristic

Figures 2 and *3* show the effect of CTS loading on curing characteristics of CTS-ENR50 and CTS-LENR50 biocomposites. *Figure 2* shows that the presence of CTS increased torque in CTS-ENR50 and CTS-LENR50 biocomposites. Increase in maximum torque as measured from the rheographs indicate that processability of biocomposites is adversely affected by the introduction of CTS. Noticeable increase in maximum torque with increasing CTS loadings can be explained by postulating that presence of fillers in the rubber matrix reduces mobility of the rubber's macromolecular chains¹⁸. Besides that, an increase of CTS loading produces biocomposites which are harder, stiffer and stronger, reflecting the enhancement in torque. Increment in stabilisation torques with an increment of CTS loading is due to CTS agglomeration which restricts the flow ability of the polymer melt. However, the

increase in LENR50 with CTS loading is not very significant compared to that in ENR50. This is attributed to the plasticising nature of polymer¹⁹. At a lower molecular weight, rubber tends to have more particle-particle interactions with CTS which allows higher loading and reduces the resistance to flow. Since the increase in torque is due to reduced chain mobility, addition of equivalent amounts of filler will be less effective in decreasing mobility of short chains.

Also depicted in *Figure 2* is the M_H - M_L (maximum torque - minimum torque), torque difference which is an indication of shear dynamic modulus corresponding to crosslink density of the compounds. Henceforth, it can be mentioned that incorporation of CTS reinforces the rubber compound and therefore increases the modulus (*Figure 2*). On the other hand, the incorporation of CTS in LENR50 did not influence stiffness of the compounds.

Cure time (t_{90}) of CTS-ENR50 and CTS-LENR50 are depicted in *Figure 3*. Based on data we can deduce that the cure time reduced as CTS was introduced in ENR50 and LENR50. The t_{90} of the compounds reduced quite sharply with 5 p.h.r. loading of CTS. The reduced cure time is an indication of an increased cure rate of the biocomposites. This is a contribution from the amine moiety in the CTS structure because it is known that amine containing compounds facilitate the curing reaction of ENR²⁰. Mixing temperature is also likely to be one of the reasons for a shorter cure time as the temperature for blending was 80°C. At this temperature, rubber-based compounds tend to undergo premature curing which results in a shorter cure time. In addition, the heat generated during blending in the internal mixer could contribute to this as well. Further addition of CTS did not affect the cure time due to processability of the blend which is not affected by addition of CTS. The cure time of LENR50 is much lower than that

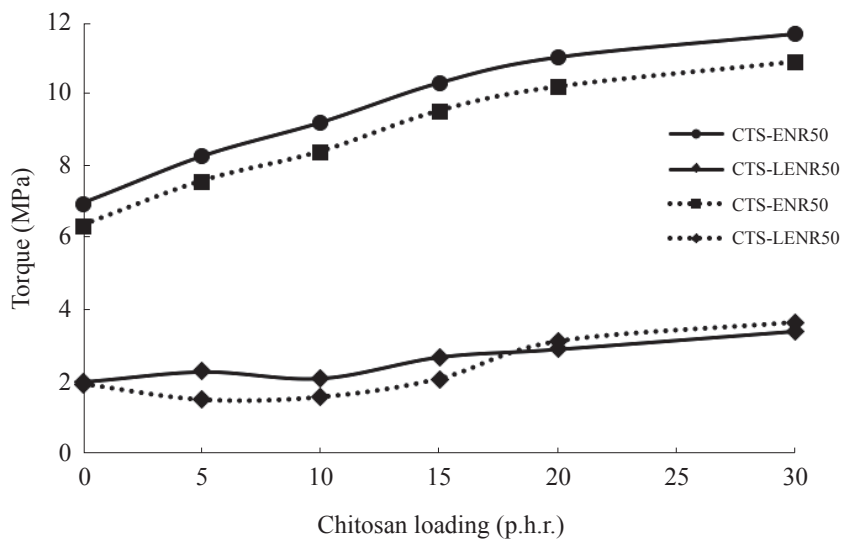


Figure 2. Effect of chitosan loading on the maximum torque and differences in torque of the rubber biocomposites.

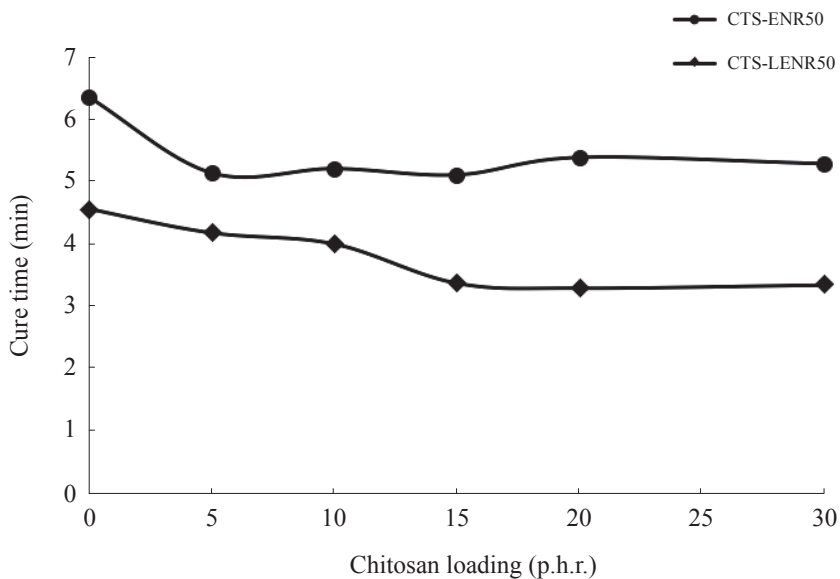


Figure 3. Effect of chitosan loading on cure time of rubber biocomposites.

of ENR50. This result is expected because molecular weight of LENR is quite low and therefore does not contribute effectively in the crosslinking network. During mixing of LENR50 and CTS, the low shear force achieved is one of the reasons for it to not cure completely unlike the networks obtained in ENR50. Further addition of CTS to LENR50 did not impart any considerable change in the cure time as maximum crosslinks had been formed.

Tensile Properties

Figures 4 to 6 depict the effect of CTS loading on tensile properties of CTS-ENR50 and CTS-LENR50 biocomposites. With the incorporation of CTS in ENR50, an initial increase in tensile strength was observed until 15 p.h.r. loading (*Figure 4*). This is possibly attributed to the improvement in adhesion between the filler-polymer matrices in the presence of CTS as shown in SEM micrographs (*Figures 7c and 8b*). Tensile strength increased with increasing filler loading until a maximum point was reached whereby the filler particles were no longer adequately separated or wetted by the rubber phase⁷. The improved filler-matrix wetting would result in reduced interfacial regions and stronger interfacial bonds. Therefore, more efficient stress transfer would occur between CTS as a load was applied. However, beyond 15 p.h.r. of CTS, a gradual reduction in tensile strength of the composite was observed. A further increase in CTS loadings had a deleterious effect on tensile strength. This is because eventually a level is reached whereby the filler particles or aggregates are no longer equally separated or wetted by the polymer matrix⁸. Thus, reduction in strength is suggested due to agglomeration of filler particles to form a domain that acts like a foreign body. ENR50 shows a higher tensile strength due to the ability of the polymer backbone to undergo strain-induced

crystallisation compared to that of LENR50. The effect of CTS loading is not as pronounced in the case of LENR50. Based on *Figure 4*, incorporation of CTS did not significantly affect tensile strength of the matrix. This was expected as molecular weight of LENR50 is too low to vulcanise and contribute effectively in the crosslink network, leading to poor tensile strength²¹. Lack of crystallisation in the vulcanisates upon stretching is one of the reasons LENR50 has lower strength compared to ENR50. Physical strength of ENR50 decreases upon depolymerisation and LENR50 displays viscous properties rather than elastic properties. The SEM micrographs (*Figure 9*) show the presence of cavities left by displacement of CTS particles from the matrices of rubber biocomposites. This indicates that interactions between CTS and natural rubber derivatives are weak.

Figure 5 shows elongation at break of CTS-ENR50 and CTS-LENR50 biocomposites. Addition of CTS to both ENR50 and LENR50 was found to reduce the elongation at break gradually. Crosslink density actually determines mechanical properties of a rubber. It is well known that modulus increases consistently with crosslink density and with that, the network turns out to be more elastic. This is the why ENR50 has a higher elongation at break than LENR50²². Presence of the carbonyl group and other side groups in LENR50 also restricts flexibility of rubber chains and leads to harder rubber composites. This could also be the reason behind lower elongation at break of LENR50 compared with ENR50.

It can be seen in *Figure 6* that modulus at 100% shows a gradual increase with CTS loading in ENR50 but only a slight improvement in the case of LENR50. Such a trend indicates that incorporation of CTS into ENR50 and LENR50 matrices increases stiffness of the corresponding biocomposite.

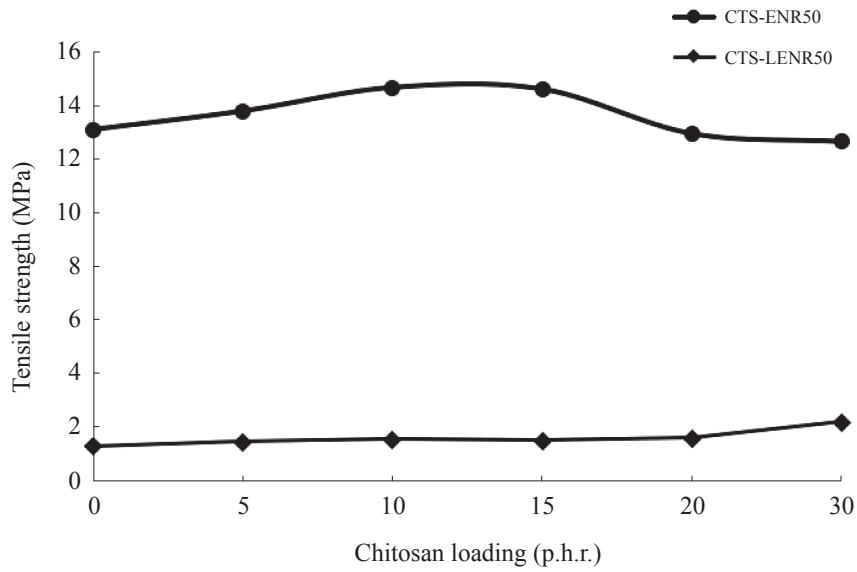


Figure 4. Effect of chitosan loading on tensile strength of rubber biocomposites.

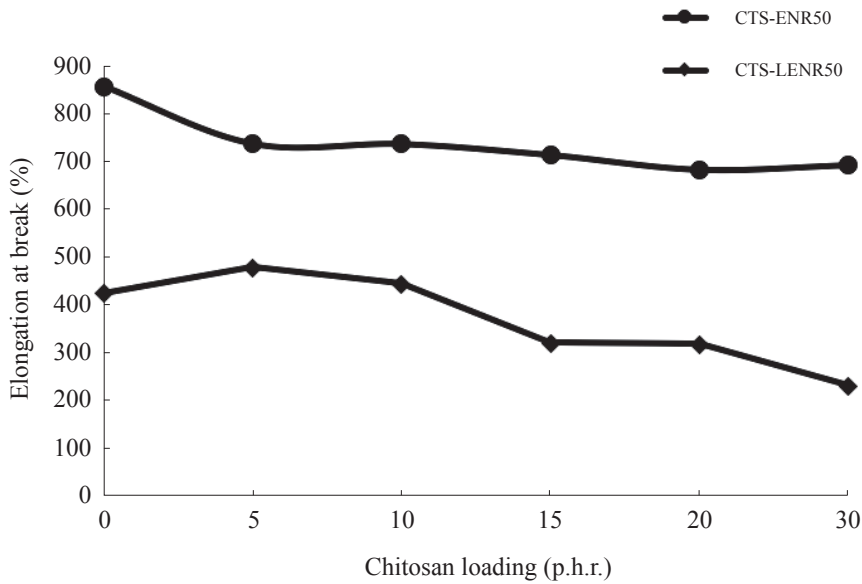


Figure 5. Effect of chitosan loading on elongation at break of rubber biocomposites.

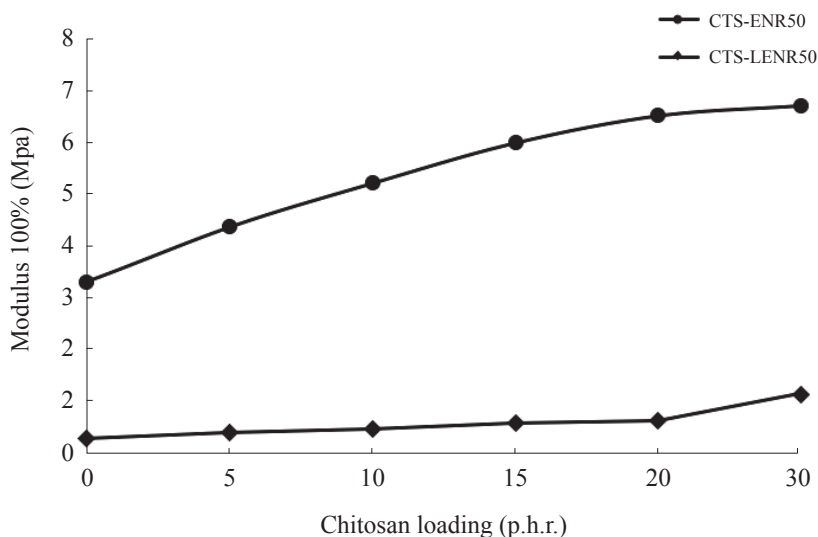


Figure 6. Effect of chitosan loading on modulus at 100% elongation of rubber biocomposites.

Higher crosslink density and good distribution of CTS in ENR50 matrices attributes to the increment in modulus at 100%. However, modulus at 100% for LENR50 is slightly influenced by addition of CTS. Nevertheless, the increase is not as significant as in ENR50 biocomposites, due to molecular entanglement within the rubber matrix itself. ENR50 has a higher molecular entanglement due to its molecular weight and this gives it a higher modulus in the first place.

Surface Morphology

SEM micrographs of fractured surfaces of CTS, CTS-ENR50 biocomposites with 0, 15 and 30 p.h.r. CTS loadings are shown in *Figures 7* and *8*, respectively. The fractured surfaces (*Figures 7b, c* and *d*) of the biocomposites are smoother suggesting good interfacial interaction between CTS and ENR. Further, it also provides direct evidence for the presence of irregular shaped CTS as shown in *Figure 7a*, which leads to poor strength properties

of the biocomposites at higher CTS loadings. *Figure 8b* shows CTS breakage rather than pull out which indicates better interfacial strength. *Figures 9a, b* and *c* illustrate the SEM micrographs of tensile fractured surfaces of CTS-LENR50 biocomposites with 0, 15 and 30 p.h.r. CTS loadings, respectively. *Figures 9b* and *c* show that the fractured surface appears smooth where CTS particles are in an infused state. This micrograph also indicates that breakage takes place at the weakest part as reflected by tensile strength.

Thermogravimetric Analysis (TGA)

The thermogravimetric (TG) and derivative thermogravimetric (DTG) curves of CTS, CTS-ENR50 and CTS-LENR50 biocomposites with CTS loadings of 0, 10 and 30 p.h.r. are depicted in *Figures 10* and *11*. From these curves, it can be seen that all biocomposites have a two-step degradation process with rapid weight loss of 80% in the temperature region of 340 – 440°C. The TG curve of CTS also

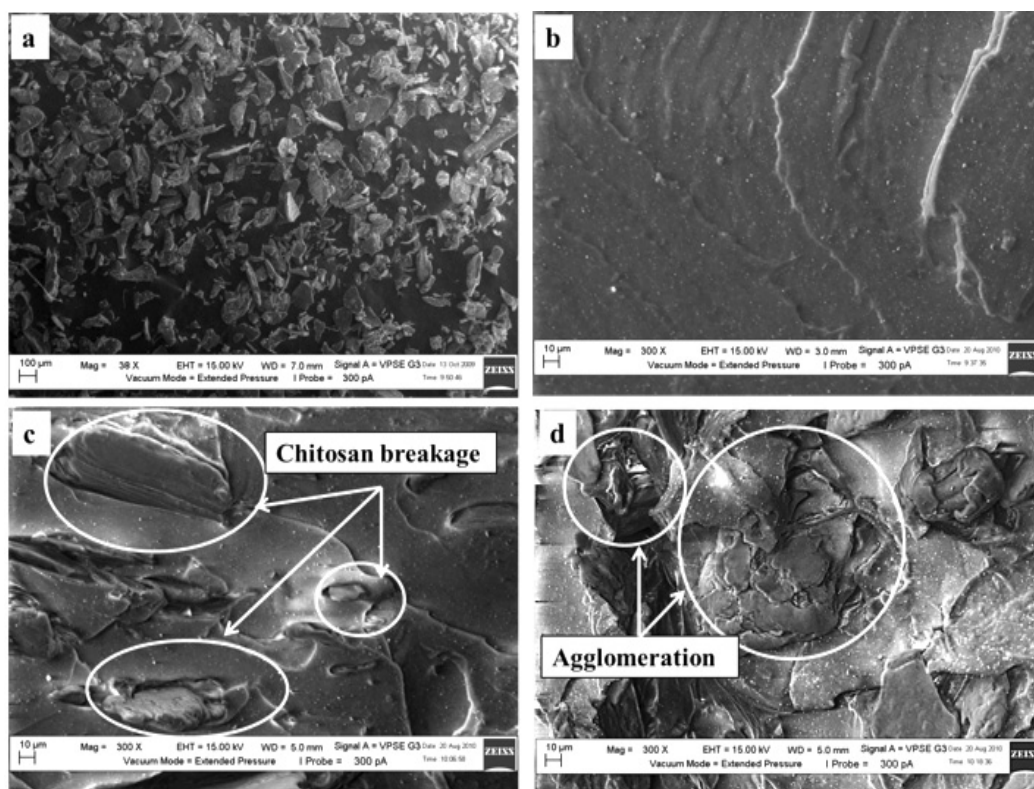


Figure 7. SEM micrographs of CTS-ENR50 biocomposites (a) SEM micrograph of Chitosan taken at a magnification of $38\times$. (b) SEM micrograph of tensile fractured surfaces of unfilled ENR50 taken at a magnification of $300\times$. (c) SEM micrograph of tensile fractured surfaces of CTS-ENR50 at 15 p.h.r. CTS loading taken at a magnification of $300\times$ (d) SEM micrograph of tensile fractured surfaces of CTS-ENR50 at 30 p.h.r. CTS loading taken at a magnification of $300\times$.

exhibits mass loss at two stages. The initial loss occurs within the range of $40 - 240^{\circ}\text{C}$ with a mass loss of 12% which corresponds to loss of water and other volatile substances. The second stage shows a mass loss of about 52% which occurs in the range of $240 - 400^{\circ}\text{C}$. This is due to chain scission and subsequent weight loss of CTS²³. At $270 - 340^{\circ}\text{C}$, ENR50 and CTS degraded about 1% and 38%, respectively. Based on this information, ENR50 is more thermally stable than CTS. Addition of CTS reduces thermal stability of the rubber. Similar behaviours are observed for LENR50 and

CTS-LENR50 biocomposites. The CTS-LENR50 biocomposites show two DTG peaks which belong to chitosan and rubber respectively. The DTG peak for CTS is more distinct than that of CTS-ENR50 biocomposites suggesting that these biocomposites are phase separated due to incompatibility.

Water Uptake Study

Results of water uptake study of CTS-ENR50 and CTS-LENR50 biocomposites are

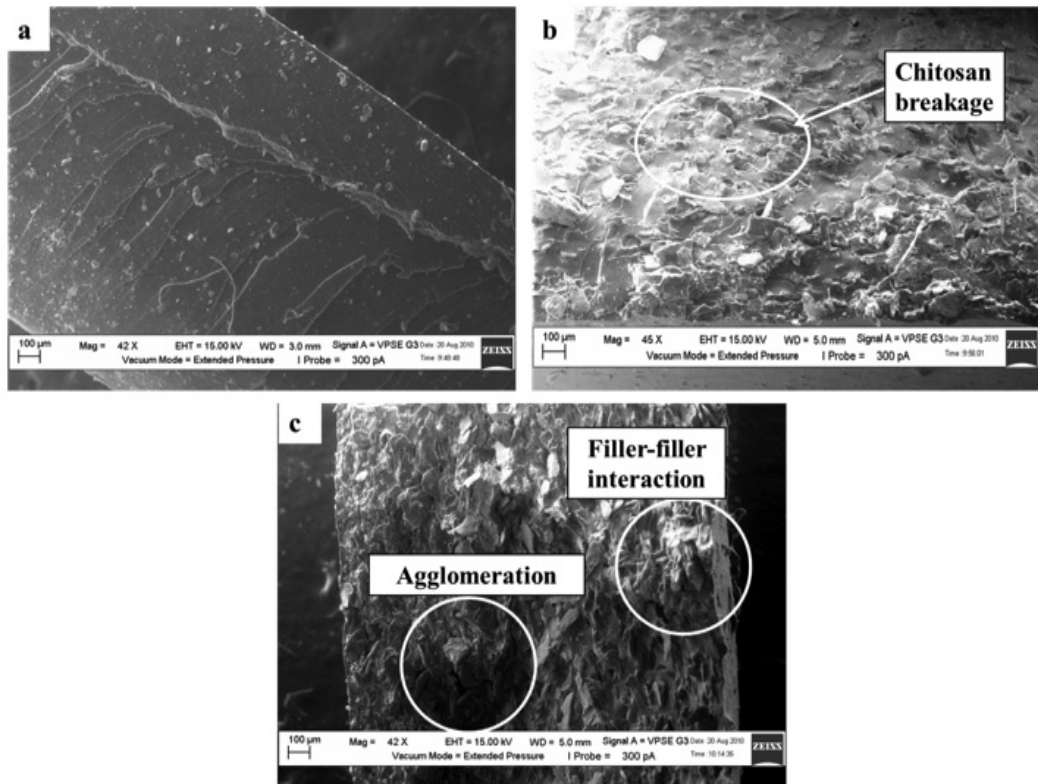


Figure 8. SEM micrographs of tensile fractured surfaces at magnification of 42 ×: (a) unfilled ENR50 (b) CTS-ENR50 at 15 p.h.r. chitosan loading (c) CTS-ENR50 at 30 p.h.r. CTS loading.

depicted in Figure 12. The results reveal that water uptake of LENR50 was higher than that of ENR50. This is attributed to presence of carbonyl functional groups at the end groups of LENR50. Carbonyl groups are hydrophilic and therefore contribute to higher uptake of water in LENR50. It is important to note that the percentage water uptake by ENR50 and LENR50 are very low compared to that of CTS (327%). This explains the increase in water uptake with increase in CTS loadings in both CTS-ENR50 and CTS-LENR50 biocomposites. It is likely that reduced crystallinity of LENR could also lead to greater water uptake. Increase in water uptake by LENR50 biocomposites could be partly

due to the presence of voids/holes (as shown in SEM micrographs in Figure 9c) which provided pathways for liquid penetration.

Toluene Absorbency

Figure 13 shows the effect of CTS loading on toluene absorbency of CTS-ENR50 and CTS-LENR50 biocomposites. It can be seen that LENR50 is a superior sorbent for toluene compared to ENR50. Moreover, the increase in CTS loading led to a decrease in toluene absorbency of both CTS-LENR50 and CTS-ENR50 biocomposites. Toluene absorbency of natural rubber derivatives is influenced by

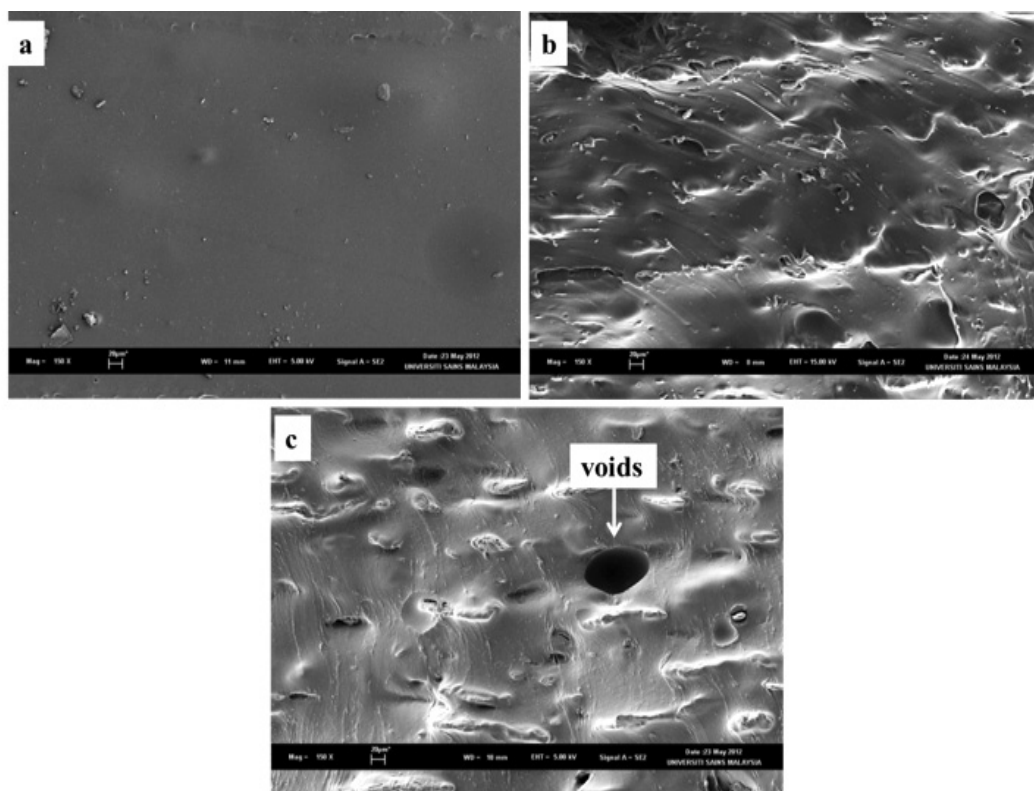


Figure 9. SEM micrographs of CTS-LENR50 biocomposites. SEM micrographs of tensile fractured surfaces at a magnification of $300\times$: (a) unfilled LENR50 (b) CTS-LENR50 at 15 p.h.r. CTS loading (c) CTS-LENR50 at 30 p.h.r. CTS loading.

factors such as types and amount of fillers. CTS is known to be insoluble in organic solvents²⁴, validating present findings whereby CTS is found to absorb only 12% of toluene. Therefore, it is probable that increasing CTS loading is equivalent to reducing ENR loading in the blend, hence toluene absorbency decreases with increasing CTS loading.

CONCLUSION

In this study, the effect of CTS loading on mechanical properties, water uptake and toluene absorbency of CTS-LENR50 and

CTS-ENR50 biocomposites were investigated. The effects were studied by observing changes in cure characteristics, tensile strength, modulus at 100% and elongation at break. Results show that increase in chitosan loading caused an increase in torque value, tensile strength and modulus at 100%, while noting a decline in cure time and elongation at break for CTS-ENR50 biocomposites. Similar trends were observed for CTS-LENR50 biocomposites except for torque value and tensile strength, whereby there was no significant effect or change with increase in chitosan loadings. Results of the water uptake study revealed that water uptake of LENR50

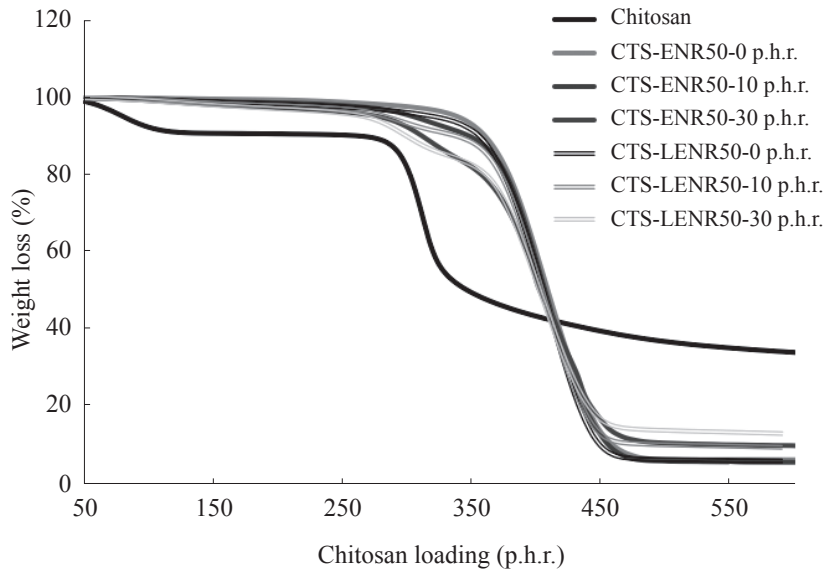


Figure 10. Effect of chitosan loading on TG plots of CTS-ENR50 and CTS-LENR50 biocomposites.

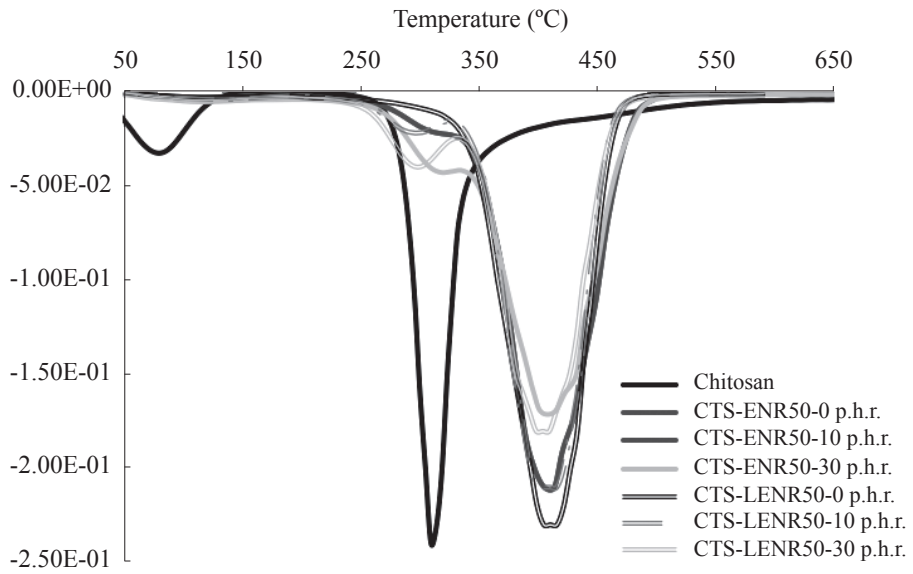


Figure 11. Effect of chitosan loading on DTG plots of CTS-ENR50 and CTS-LENR50 biocomposites.

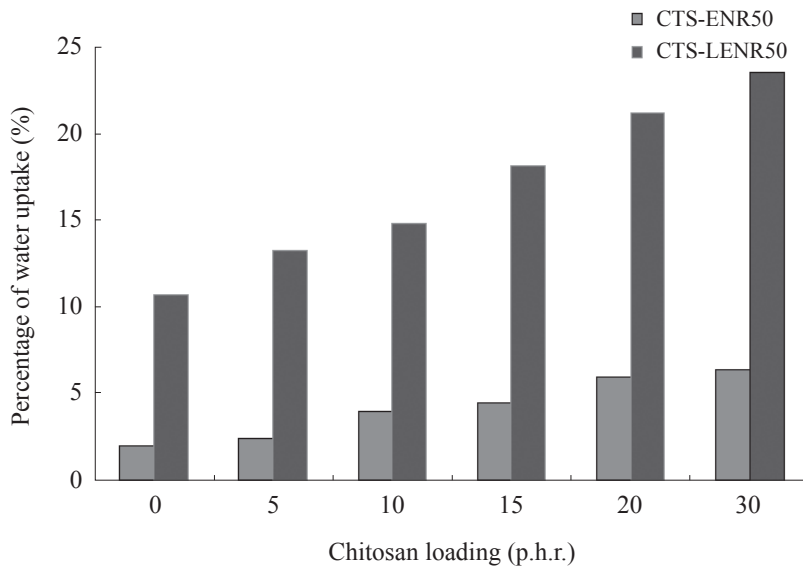


Figure 12. Effect of chitosan loading on water uptake of rubber biocomposites.

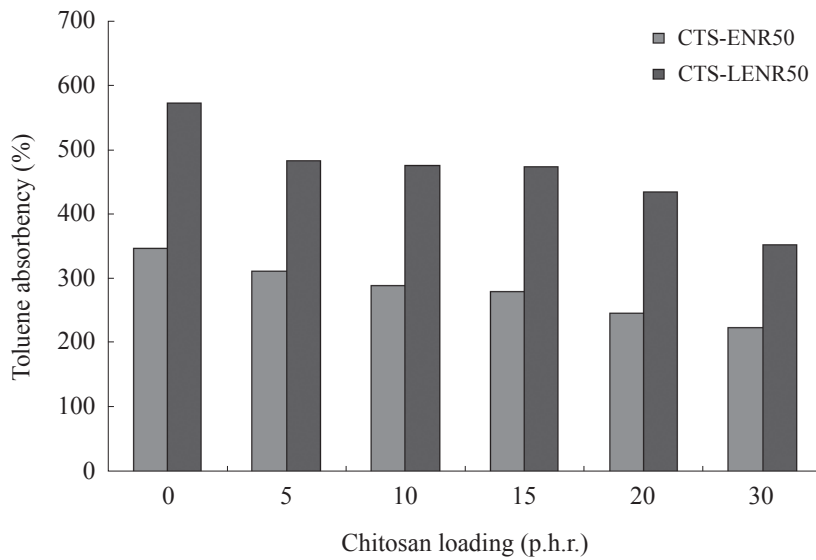


Figure 13. Effect of chitosan loading on toluene absorbency of rubber biocomposites.

was at least four folds higher than that of ENR50, and increase in CTS loadings caused an increase in water uptake in CTS-ENR50 and CTS-LENR50 biocomposites. Results of the toluene absorbency study revealed that LENR50 was a superior sorbent for toluene compared to ENR50, but increase in CTS loadings led to decrease in toluene absorbency for both CTS-LENR50 and CTS-ENR50 biocomposites.

ACKNOWLEDGEMENTS

The authors would like to thank Universiti Sains Malaysia (USM) for providing financial support, Research University (RU) grants no. 1001/PKIMIA/814124 and PRGS 1001/PKIMIA/842021. Gunasunderi Raju is also grateful to Malaysian Rubber Board for the fellowship scheme in pursuing her PhD.

Date of receipt: November 2012

Date of acceptance: May 2013

REFERENCES

1. BAKER, C.S.L., GELLING, I.R. AND SAMSURI, A. (1986) Epoxidised Natural Rubber. *J. nat. Rubb. Res.*, **1**, 135–144.
2. GAN, S.N. AND HAMID, Z.A. (1997) Partial Conversion of Epoxide Groups to Diols in Epoxidized Natural Rubber. *Polym.* **38**, 1953–1956.
3. HEPING, Y., SIDONG, L. AND ZHENG, P. (1999) Preparation and Study of Epoxidized Natural Rubber. *J. Therm. Anal. Calorim.*, **58**, 293–299.
4. HAMZAH, R., ABU BAKAR, M., KHAI-RUDDEAN, M., AHMED MOHAMMED, I. AND ADNAN, R. (2012) A Structural Study of Epoxidized Natural Rubber (ENR-50) and its Cyclic Dithiocarbonate Derivative using NMR Spectroscopy Techniques. *Molecules*, **17**, 10974–10993.
5. GAZELEY, K. F. AND MENTE, P. G. (1986) Method for Reducing the Molecular Weight of Rubber in Latex. United Kingdom Patent 2183663.
6. ISMAIL, H., ROZMAN, H.D., JAFFRI, R.M. AND MOHD, Z.A. (1997) Oil Palm Wood Flour Reinforced Epoxidized Natural Rubber Composites: The Effect of Filler Content and Size. *Eur. Polym. J.*, **33**, 1627–1632.
7. ISHAK, Z.A.M. AND BAKAR, A.A. (1995) An Investigation on the Potential of Rice Husk Ash as Fillers for Epoxidized Natural Rubber (ENR). *Eur. Polym. J.*, **31**, 259–269.
8. PAL, K., RAJASEKAR, R., KANG, D.J., ZHANG, Z.X., KIM, J.K. AND DAS, C.K. (2009) Effect of Epoxidized Natural Rubber-organoclay Nanocomposites on NR/high Styrene Rubber Blends with Fillers. *Mater. Design.*, **30**, 4035–4042.
9. DEROUET, D., BROSE, J.C. AND TILLEKERATNE, L.M.K. (1990) Fixation of Methacrylic Acid onto Epoxidised Liquid Natural Rubber. *J. nat. Rubb. Res.*, **5**, 296–300.
10. PERERA, M.C.S. (1990) Reaction of Aromatic Amines with Epoxidized Natural Rubber Latex. *J. Appl. Polym. Sci.*, **39**, 749–758.
11. HASHIM, A.S. AND KOHJIYA, S. (1994) Curing of Epoxidized Natural Rubber with p-phenylenediamine. *J. Polym. Sci. Part A: Polym. Chem.*, **32**, 1149–1157.
12. CHANDRA, R. AND RUSTGI, R. (1998) Biodegradable Polymer. *Prog. Polym. Sci.*, **23**, 1273.
13. DUTTA, P.K., DUTTA, J. AND TRIPATHI, V.S. (2004) Chitin and Chitosan: Chemistry, Property and Application. *J. Sci. Ind. Res.*, **63**, 20–31.
14. LERTWATTANASERI, T., MIZOGUCHI, N.T., TANAKA, Y. AND CHIRACHAN-CHAI, S. (2009) Epoxidized Natural

- Rubber Bionanocomposite: A Model Case of Bionanocomposite Using Nanofibrous Chitosan and its Consequent Functional Properties. *Chem. Lett.*, **38**, 798.
15. SHAARI, S.M., ISMAIL, H. AND OTHMAN, N. (2011) The Effect of Chitosan Loading on the Properties of Chitosan Filled Epoxidized Natural Rubber Compounds. *Key Eng. Mater.*, **471–472**, 851–856.
 16. ISMAIL, H., SHAARI, S.M. AND OTHMAN, N. (2011) The Effect of Chitosan Loading on the Curing Characteristics, Mechanical and Morphological Properties of Chitosan-filled Natural Rubber (NR), Epoxidised Natural Rubber (ENR) and Styrene-butadiene Rubber (SBR) Compounds. *Polym. Test.*, **30**, 784–790.
 17. MALZ, F. AND JANCKE, H. (2005) Validation of Quantitative NMR. *J. Pharma. Biomed. Anal.*, **38**, 813–823.
 18. DA COSTA H.M., VISCONTE, L.L.Y., NUNES, R.C.R. AND FURTADO, C.R.G. (2000) The Effect of Coupling Agent and Chemical Treatment on Rice Husk Ash-filled Natural Rubber Composites. *J. Appl. Polym. Sci.*, **76**, 1019.
 19. RADHAKRISHNAN, N.N., THOMAS, S. AND MATHEW, N. (1997) Liquid Natural Rubber as a Viscosity Modifier in Nitrile Rubber Processing. *Polym. Int.*, **42**, 289–300.
 20. MOUSA, A. AND KARGER-KOCSIS, J. (2001) Rheological and Thermodynamical Behavior of Styrene/butadiene Rubber-organoclay Nanocomposites. *Macromol. Mater. Eng.*, **286**, 260 – 266.
 21. DULNGALI, S. AND MAIDUNNY, Z. A. (1991) Liquid Natural Rubber, Paper Presented at the Seminar Kebangsaan Menilai Pencapaian Penyelidikan IRPA dalam Rancangan Malaysia Ke-5 Sektor Perindustrian, Universiti Utara Malaysia, Kedah, 20-24 Disember 1991.
 22. HUSSIN, M. AND EBDON, J.R. (1998) Telechelic Liquid Natural Rubber: A Review. *Prog. Polym. Sci.*, **23**, 143–177.
 23. PAWLAK, A. AND MUCHA, M. (2003) Thermogravimetric and FTIR Studies of Chitosan Blends. *Thermochim. Acta*, **396**, 153–166.
 24. RANGRONG, Y., MICHIIYA, M., MITSURU, A. AND SUWABUN, C. (2004) Controlled Hydrophobic/hydrophilic Chitosan: Colloidal Phenomena and Nanosphere Formation. *Colloid Polym. Sci.*, **282**, 337–342.